

# Smart Multifunctional Hollow Microspheres for the Quick Release of Drugs in Intracellular Lysosomal Compartments\*\*

Cherng-Jyh Ke, Tzu-Yuan Su, Hsin-Lung Chen, Hao-Li Liu, Wei-Lun Chiang, Po-Chun Chu, Younan Xia,\* and Hsing-Wen Sung\*

Poly(D,L-lactic-co-glycolic acid) (PLGA) has been widely used as a carrier material for drug release owing to its excellent biocompatibility and biodegradability.<sup>[1–3]</sup> The loaded drug is typically released through diffusion and/or polymer degradation.<sup>[4–6]</sup> However, the degradation process can take days or even months, so that drug release from PLGA-based carriers is often a slow process.<sup>[4]</sup> As a result, the concentration of a drug released from PLGA-based carriers may not be able to reach the therapeutic threshold promptly. Herein we report a novel smart system based on PLGA hollow microspheres (HMs) that can deliver an anti-cancer drug into tumor cells and quickly release the drug in an acidic organelle, such as a lysosome. The key component of this system is sodium bicarbonate ( $\text{NaHCO}_3$ ), which can be readily incorporated into HMs together with an anti-cancer drug by the use of a double-emulsion method. In an acidic environment,  $\text{NaHCO}_3$  reacts with the acid to quickly generate  $\text{CO}_2$  bubbles,<sup>[7]</sup> which cause the microsphere wall to burst and thereby swiftly release the anticancer drug.

It is known that mammalian tissues are bathed in a milieu that typically contains  $\text{HCO}_3^-$  at a con-

centration of about 25 mM, and cells have developed a mechanism to take up extracellular  $\text{HCO}_3^-$  to neutralize their cytosol.<sup>[8]</sup> The physiological pH value of body fluid (or the extracellular environment) is 7.4, whereas that in the

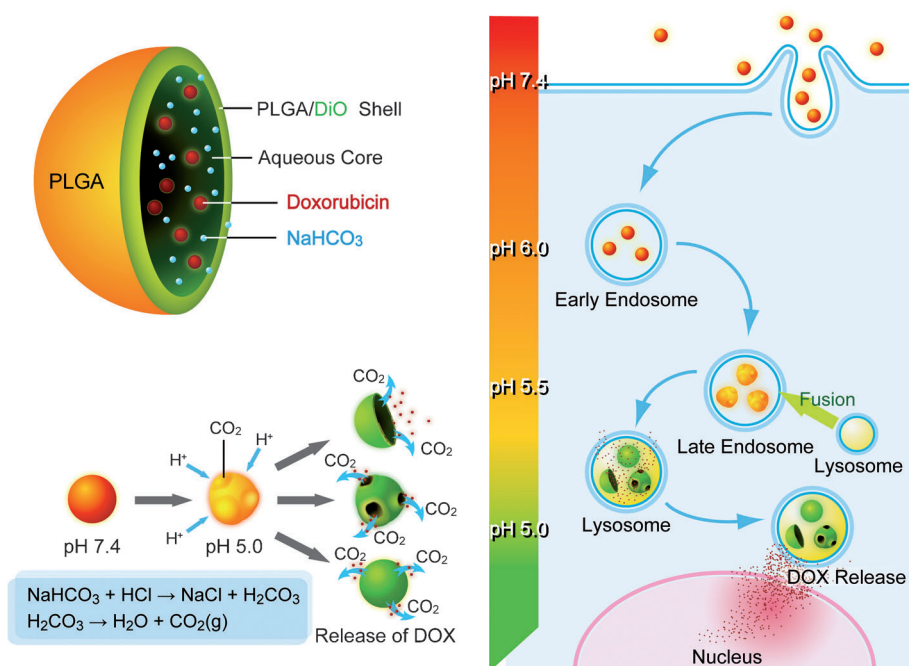


**Figure 1.** Schematic illustration of the structure of a PLGA hollow microsphere containing doxorubicin and the mechanism of drug release (left), as well as the intracellular trafficking and release of the drug from the pH-responsive microspheres (right).

intracellular early endosomes and late endosomes/lysosomes is around 6.0 and 5.0, respectively.<sup>[8,9]</sup> Figure 1 shows a schematic illustration of the smart system and how it works. We used PLGA as a typical example to demonstrate the concept with the notion that the same approach can be extended to other biodegradable polymers. To help track the particles intracellularly, we doped the PLGA shells of HMs with DiO, a lipophilic dye. We used doxorubicin (DOX) as an example of an anticancer drug, because it has fluorescence capability and has been widely used in the treatment of a broad spectrum of tumors. Owing to DOX-related acute cardiotoxicity and multidrug resistance of cancer cells, the development of an advanced delivery system for DOX is highly desired.<sup>[10,11]</sup> In this study, DOX was encapsulated in the aqueous core of HMs by physical means, as opposed to covalent attachment, which may alter the activity of the drug.<sup>[10]</sup> Once an HM has been transported into an endocytic

[\*] C. J. Ke, T. Y. Su, Prof. H. L. Chen, W. L. Chiang, Prof. H. W. Sung  
Department of Chemical Engineering  
National Tsing Hua University, Hsinchu, Taiwan 30013 (ROC)  
E-mail: hwsung@che.nthu.edu.tw

Prof. H. L. Liu, P. C. Chu  
Department of Electrical Engineering, Chang-Gung University  
Taoyuan, Taiwan 33302 (ROC)

Prof. Y. Xia  
Department of Biomedical Engineering, Washington University  
St. Louis, MO 63130 (USA)  
E-mail: xia@biomed.wustl.edu

[\*\*] This research was supported by a grant from the National Science Council (NSC 99-2120-M-007-007). We thank Yu-Tung Chen for assistance with the schematic drawings.

Supporting information for this article is available on the WWW under <http://dx.doi.org/10.1002/ange.201102852>.

organelle of a live cell, the protons ( $H^+$ ) infiltrating from the compartment react with the  $NaHCO_3$  contained in an HM to generate  $CO_2$  gas. The evolving  $CO_2$  bubbles cause the shell to rupture owing to the increase in internal pressure. As a result, by incorporating  $NaHCO_3$  in the aqueous core, we were able to obtain a class of smart carriers that could promptly unload the encapsulated drug at a selected intracellular site by taking advantage of the differences in subcellular pH value.

Besides the smartness in drug release, this new delivery system has the advantages of the green fluorescence of DiO in the PLGA shell and red fluorescence of DOX in the aqueous core upon excitation at 488 nm for the purposes of tracking and monitoring. As expected, the pristine HMs appeared orange owing to merging of the green (DiO) and red (DOX) fluorescence, and the color gradually changed from orange to yellow and then green during the course of DOX release. Thus, this dual-emission system enabled us to localize the HMs and monitor DOX release intracellularly.

The smart HMs were prepared by a double-emulsion method in the presence of  $NaHCO_3$  at different concentrations (0, 1.25, 2.5, and 5.0  $mg\ mL^{-1}$ ). These concentrations are comparable to those commonly used for the preparation of a buffer for cell culture. The as-prepared HMs were collected by centrifugation and washed with deionized (DI) water. Scanning electron microscopy (SEM) showed that the particles were spherical in shape with a smooth surface, except for the sample prepared with  $NaHCO_3$  at a concentration of 5.0  $mg\ mL^{-1}$  (Figure 2a). In this case, pores were clearly observed on the surface of some particles. Since these porous HMs were unable to hold DOX, they were not used in subsequent studies. The as-prepared HMs could be redispersed in water without the formation of any aggregates. They had a  $\zeta$  potential of  $-2.5$  mV, and their diameters varied from 1 to 3  $\mu m$ . A TEM micrograph of a particle from a sample prepared in the absence of  $NaHCO_3$  clearly revealed its hollow structure (Figure 2b). The PLGA shell had a thickness of 100–200 nm. The distributions of DiO in the PLGA shell and DOX in the aqueous core of a microsphere were confirmed by fluorescence microscopy (Figure 2c). Lipid-soluble DiO (green fluorescence) was chosen because it only

entered the hydrophobic PLGA shell instead of the aqueous core; in contrast, DOX (red fluorescence) was mainly present in the aqueous core. When the images were combined, an orange color was observed as a result of the superposition of the green and red fluorescence.

All HMs containing  $NaHCO_3$  had a smooth surface and a dense morphology at pH 7.4 (Figure 3; see also Figure S1 in the Supporting Information). In contrast, some HMs were

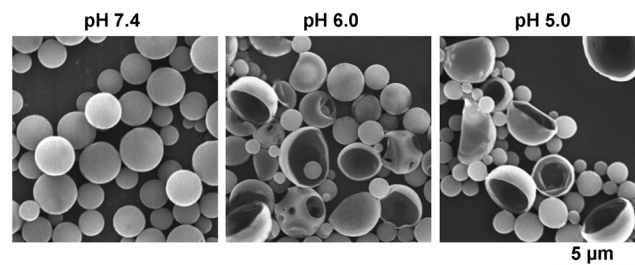


**Figure 3.** SEM micrographs of HMs after incubation in media with different pH values to mimic the extracellular environment (pH 7.4), early endosomes (pH 6.0), and lysosomes (pH 5.0). The HMs were prepared with sodium bicarbonate at a concentration of 2.5  $mg\ mL^{-1}$ .

found to rupture their PLGA shells in acidic solutions (pH 6.0 and 5.0), as shown by the presence of fragments from the broken particles. The broken particles together with those that clearly showed pores on the surface accounted for approximately 30% of the sample. In the case of those HMs that remained intact, there were micropores present in their PLGA shells, but they were too small to be clearly resolved by SEM. The presence of micropores in the shells of HMs was confirmed by small-angle X-ray scattering (SAXS). A large number of  $CO_2$  bubbles were generated when the HMs containing  $NaHCO_3$  were exposed to an acidic solution (see the ultrasound images in Figure S2). After the treatment of HMs with an acidic solution, the permeability of the PLGA shells was greatly increased owing to the formation of micropores inside the shells (see Figure S3).

The encapsulation of DOX in HMs was found to be effective: 10.8% loading efficiency was observed ( $n=6$  batches). Although the free volume in the PLGA shell enables small ions, such as protons ( $H^+$ ), to quickly diffuse through the shell, such diffusion is prohibited for DOX because the relatively hydrophobic DOX molecules can form aggregates in an aqueous phase, and the shell should be impenetrable to these aggregates. As an initial test to verify the effectiveness of the as-prepared HMs for drug-delivery applications, the particles were suspended in media with different pH values of 7.4, 6.0, and 5.0. The medium was removed with a syringe at given time intervals for analysis and replaced with the same volume of fresh medium.<sup>[4]</sup> Figure 4a shows the profiles of DOX release from HMs into a phosphate buffer at 37 °C. There was essentially no release of DOX from the HMs without  $NaHCO_3$  (HMs-w/o- $NaHCO_3$ ) at different pH values, which suggests that the diffusion of DOX through the PLGA shells was rather slow and pH-independent. In contrast, the release of DOX from the HMs containing  $NaHCO_3$  in the core was pH-dependent.

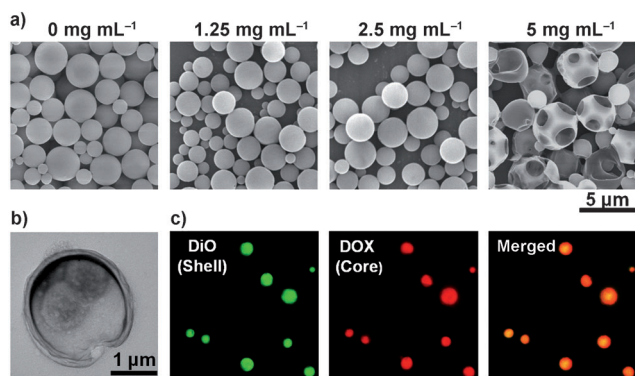


**Figure 2.** a) SEM micrographs of HMs prepared with sodium bicarbonate at different concentrations by using a double-emulsion method. b) TEM micrograph revealing the hollow structure of an HM prepared in the absence of sodium bicarbonate. c) Fluorescence micrographs of the HMs, showing the fluorescence of DiO and DOX, and superposition of the images (right).

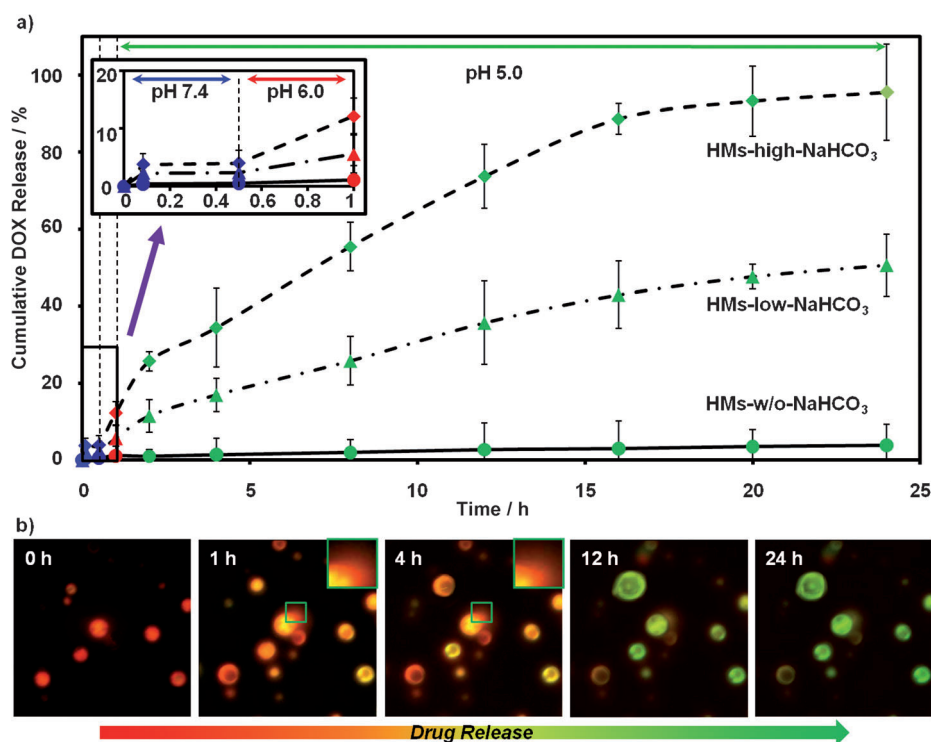


**Figure 4.** a) Release profiles of DOX for HMs incubated in media with different pH values to mimic the extracellular environment (pH 7.4), early endosomes (pH 6.0), and lysosomes (pH 5.0) at 37°C. b) Fluorescence micrographs showing the changes in color of HMs (prepared with sodium bicarbonate at 2.5 mg mL<sup>-1</sup>) during the course of DOX release.

The cumulative amount of DOX released from HMs at pH 7.4 (in the extracellular environment, in the first 30 min) and at pH 6.0 (in the early endosomes, 30–60 min) was limited. However, once the HMs reached the pH milieu of the late endosomes/lysosomes (pH 5.0, after 1 h,  $P < 0.05$ ), the release of DOX increased significantly. In these compartments, the acid led to the generation of CO<sub>2</sub> bubbles that could intrude through the PLGA shells and create small pores. The pores were large enough for the encapsulated DOX aggregates to escape through. When NaHCO<sub>3</sub> was used at a higher concentration (HMs-high-NaHCO<sub>3</sub>), a greater amount of DOX was released ( $P < 0.05$ ) within the same period of time. After incubation at pH 5 for 24 h, about 90% of the DOX originally encapsulated within HMs-high-NaHCO<sub>3</sub> was released into the medium. The observed color of the HMs by fluorescence microscopy changed from orange (superposition of green (DiO) and red (DOX)) to yellow (together with a little red fluorescence surrounding the carriers owing to the release of DOX from the HMs) to green (empty HMs with PLGA/DiO shells) during the course of DOX release (Figure 4b). This pH-sensitive release behavior is of particular interest for the intracellular delivery of DOX.

The HMs taken up by Hep3B cells were expected to experience an increasingly acidic environment as they were trafficked into the early endosomes and then into the late endosomes/lysosomes (see Figure S4). To gain a better understanding of the effect of DOX released intracellularly, we incubated the cells with various HMs for different

durations, and recorded fluorescence images by confocal laser scanning microscopy (CLSM). The carriers still appeared orange after incubation for 24 h in the case of HMs-w/o-NaHCO<sub>3</sub>, and no DOX (red fluorescence) accumulation was observed inside the cell nuclei (Figure 5). In contrast, for HMs containing NaHCO<sub>3</sub>, orange fluorescence indicative of DOX-loaded HMs was seen in the early endosomes at  $t = 1$  h after incubation, and at  $t = 4$  h, the carriers became yellow, with weak red fluorescence in their surroundings. At this point, weak red fluorescence (suggesting the accumulation of DOX) was seen inside the cell nuclei for the sample incubated with HMs-high-NaHCO<sub>3</sub>. As the incubation time progressed to 12 and 24 h, the accumulation of red fluorescence (DOX) in the cell nuclei became more apparent, whereas the intensity of green fluorescence (empty HMs) in their surrounding area became stronger. These observations were more remark-

able for HMs-high-NaHCO<sub>3</sub> than for HMs-low-NaHCO<sub>3</sub>. By 24 h after incubation, DOX had been almost completely released from HMs-high-NaHCO<sub>3</sub> and had accumulated in the cell nuclei. It is important that DOX is transported into the cell nuclei to exert its cytotoxicity because its mechanism of action is to interact with DNA by intercalation and the inhibition of macromolecular biosynthesis.<sup>[11]</sup> The results of an MTT assay (see Figure S5; MTT = 3-(4,5-dimethylthiazol-2-yl)-2,5-diphenyltetrazolium bromide) suggest that the efficient cellular uptake of HMs-high-NaHCO<sub>3</sub> and their site-specific drug release led to the buildup of an intracellular drug concentration higher than the cell-killing threshold and thus to cell death.

In summary, we have demonstrated that the release of DOX from NaHCO<sub>3</sub>-containing HMs depends on the pH level in the endocytic organelles. Once the HMs reach the lysosomal compartments, where the pH value is near 5.0, the release of DOX is triggered promptly by the formation of CO<sub>2</sub> bubbles. Such a stimuli-responsive carrier could potentially be used for the controlled release of drugs in acidic organelles. Additionally, the dual fluorescence emission of the HMs can be used for sensing/imaging drug release during the course of intracellular trafficking. The stimuli-responsive drug carriers will enable on-demand controlled release profiles that may enhance therapeutic effectiveness and reduce systemic toxicity.<sup>[12]</sup>



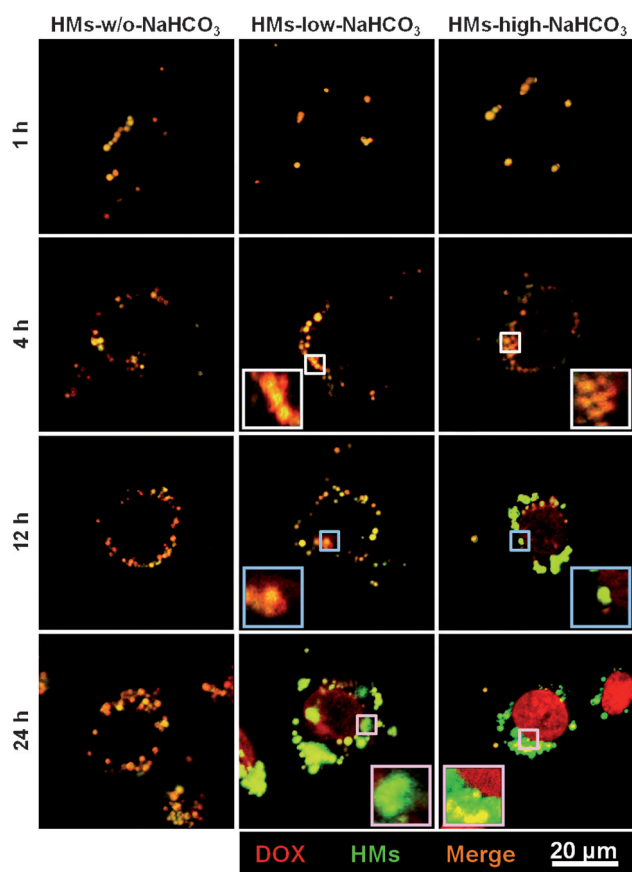


**Figure 5.** CLSM images showing the intracellular release of DOX from PLGA HMs. For HMs-w/o-NaHCO<sub>3</sub>, the color of the carriers remained the same (orange, a combination of DOX and HMs) throughout the entire course of the experiment. In contrast, the accumulation of DOX in the cell nuclei could be observed as time proceeded for the HMs containing NaHCO<sub>3</sub>, and the intensity of green fluorescence (empty HMs) in the surrounding area became stronger. The release of DOX (red fluorescence) in the lysosomal compartments from PLGA HMs (green fluorescence) increased significantly when the amount of NaHCO<sub>3</sub> incorporated was increased. Insets show a higher-magnification image of the indicated region.

### Experimental Section

**Materials:** PLGA (with a lactide/glycolide molar ratio of 75:25 and an inherent viscosity of 0.17 dL g<sup>-1</sup>) was obtained from BioInvigor (Taipei, Taiwan). DOX was purchased from Fisher Scientific (Waltham, MA, USA). Poly(vinyl alcohol) (PVA, MW ≈ 30–70 kDa), NaHCO<sub>3</sub>, dichloromethane, and 3,3'-dioctadecyloxycarbocyanine perchlorate (DiO) were all obtained from Sigma-Aldrich (St. Louis, MO, USA). All chemicals and reagents used were of analytical grade.

**Fabrication of PLGA HMs:** The HMs were prepared by using a water-in-oil-in-water (W/O/W) double-emulsion, solvent-diffusion-evaporation technique. In a typical process, aqueous PVA (10 mg mL<sup>-1</sup>, 1 mL) containing NaHCO<sub>3</sub> (0, 1.25, 2.5, or 5.0 mg mL<sup>-1</sup>) and DOX (1 mg mL<sup>-1</sup>) was emulsified with a solution of PLGA (5 mg mL<sup>-1</sup> in CH<sub>2</sub>Cl<sub>2</sub>, 2 mL) containing DiO (0.05 mg mL<sup>-1</sup>) to generate the primary W/O emulsion. The emulsification was carried out with an ultrasonicator (Sonics & Materials, Newtown, CT, USA) at 35 W for 2 min in an ice bath. The primary emulsion was then added to a PVA solution (6 mL) without NaHCO<sub>3</sub>

and homogenized at 5000 rpm for 30 min in an ice bath by using a Polytron PT-1200 Homogenizer (Kinematic AG, Littau, Switzerland) to produce the W/O/W double emulsion. The double emulsion was transferred into deionized water (30 mL) and stirred overnight at room temperature to evaporate all of the CH<sub>2</sub>Cl<sub>2</sub>. The solidified HMs were collected by centrifugation (1500 rpm, 30 min), washed three times with deionized water, and finally resuspended in deionized water (10 mL).

**In vitro drug-release study:** The profiles for the in vitro release of DOX from HMs were established by dialysis of the DOX-loaded particle suspensions in phosphate-buffered saline (PBS) with different pH values in the dark. Briefly, 2 mL aliquots of the DOX-loaded HM suspensions (50 μg mL<sup>-1</sup>) were dialyzed against 15 mL of the buffer (molecular-weight cutoff: 12000–14000) and gently shaken in a thermostatic rotary shaker at 100 rpm and 37°C. Samples were removed at different intervals, and an equal amount of the same medium was added to maintain a constant volume. The amount of DOX released from the HMs was analyzed by using a fluorescence spectrometer.

**Intracellular sensing/imaging of drug release:** To monitor the drug release from various HMs intracellularly, Hep3B cells were treated with DOX-loaded particles in a serum-free medium. After incubation for predetermined periods of time, the cells were washed twice with prewarmed PBS and then fixed in 4% paraformaldehyde. The fixed cells were then examined by CLSM.

**Statistical analysis:** Two groups were compared by the one-tailed Student *t* test by using statistical software (SPSS, Chicago, IL, USA). Data are presented as the mean ± standard deviation. A difference of *P* < 0.05 was considered statistically significant.

Received: April 25, 2011

Revised: June 14, 2011

Published online: July 12, 2011

**Keywords:** controlled release · drug delivery · double emulsions · fluorescence · multifunctional particles

- [1] A. G. Ding, A. Shenderova, S. P. Schwendeman, *J. Am. Chem. Soc.* **2006**, *128*, 5384.
- [2] A. A. van Apeldoorn, H.-J. van Manen, J. M. Bezemer, J. D. de Bruijn, C. A. van Blitterswijk, C. Otto, *J. Am. Chem. Soc.* **2004**, *126*, 13226.
- [3] S. W. Choi, Y. Zhang, Y. Xia, *Angew. Chem.* **2010**, *122*, 8076; *Angew. Chem. Int. Ed.* **2010**, *49*, 7904.
- [4] B. S. Zolnik, D. J. Burgess, *J. Controlled Release* **2007**, *122*, 338.
- [5] M. L. Ho, Y. C. Fu, G. J. Wang, H. T. Chen, J. K. Chang, T. H. Tsai, C. K. Wang, *J. Controlled Release* **2008**, *128*, 142.
- [6] K. Na, S. Kim, K. Park, K. Kim, D. G. Woo, I. C. Kwon, H.-M. Chung, K.-H. Park, *J. Am. Chem. Soc.* **2007**, *129*, 5788.
- [7] B. Y. Choi, H. J. Park, S. J. Hwang, J. B. Park, *Int. J. Pharm.* **2002**, *239*, 81.
- [8] J. R. Casey, S. Grinstein, J. Orlowski, *Nat. Rev. Mol. Cell Biol.* **2010**, *11*, 50.
- [9] K. Miyata, M. Oba, M. Nakanishi, S. Fukushima, Y. Yamasaki, H. Koyama, N. Nishiyama, K. Kataoka, *J. Am. Chem. Soc.* **2008**, *130*, 16287.
- [10] F. Tewes, E. Munnier, B. Antoon, L. Ngaboni Okassa, S. Cohen-Jonathan, H. Marchais, L. Douziech-Eyrolles, M. Soucé, P. Dubois, I. Chourpa, *Eur. J. Pharm. Biopharm.* **2007**, *66*, 488.
- [11] S. Cai, S. Thati, T. R. Bagby, H.-M. Diab, N. M. Davies, M. S. Cohen, M. L. Forrest, *J. Controlled Release* **2010**, *146*, 212.
- [12] B. P. Timko, T. Dvir, D. S. Kohane, *Adv. Mater.* **2010**, *22*, 4925.